Journal of Visualized Experiments

Electric and magnetic field devices for stimulation of biological tissues

--Manuscript Draft--

Article Type:	Methods Article - Author Produced Video
Manuscript Number:	JoVE62111R1
Full Title:	Electric and magnetic field devices for stimulation of biological tissues
Corresponding Author:	Juan Vaca-Gonzalez, Ph.D. Fundacion Universitaria del Area Andina COLOMBIA
Corresponding Author's Institution:	Fundacion Universitaria del Area Andina
Corresponding Author E-Mail:	jvaca8@areandina.edu.co
Order of Authors:	Juan José Saiz Culma
	Juan Felipe Escobar Huertas
	Diego Alexander Garzón-Alvarado
	Juan Vaca-Gonzalez, Ph.D.
Additional Information:	
Question	**Response**
Please specify the section of the submitted manuscript.	Bioengineering
Please indicate whether this article will be Standard Access or Open Access.	Standard Access (US$1200)
Please confirm that you have read and agree to the terms and conditions of the author license agreement that applies below:	I agree to the Author License Agreement
Please provide any comments to the journal here.	

jove JOURNAL OF VISUALIZED EXPERIMENTS
1 Alewife Center #200
Cambridge, MA 02140
tel. 617.945.9051
www.jove.com

Standard Manuscript Template
Remove all gray text before submitting

TITLE:
Electric and magnetic field devices for stimulation of biological tissues.

AUTHORS AND AFFILIATIONS:
Juan José Saiz Culma[1,2], Juan Felipe Escobar Huertas[3], Diego Alexander Garzón-Alvarado[1,2], Juan Jairo Vaca-González[4,]

[1] Biomimetics Laboratory, Instituto de Biotecnología, Universidad Nacional de Colombia, Bogota, Colombia
[2] Numerical Methods and Modeling Research Group (GNUM), Universidad Nacional de Colombia, Bogota, Colombia
[3] Design, Analysis and Development of Engineering Systems Research group (GIDAD), Fundación Universitaria Los Libertadores, Bogota, Colombia
[4] School of Health and Sports Sciences, Fundación Universitaria del Área Andina, Bogota, Colombia

jjsaizc@unal.edu.co
juanfe977@gmail.com
dagarzona@unal.edu.co

All authors contributed to the design of the study, simulation of electric and magnetic fields, manufacture of electrical and magnetic stimulators, analysis and interpretation of the data, drafting and revision of the manuscript and approval of final version of the manuscript.

Corresponding author:
Juan Jairo Vaca-González: jvaca8@areandina.edu.co

KEYWORDS:
Electric Field, Magnetic Field, Biophysical stimuli, Stimulator, Biological tissue.

SUMMARY:
This protocol describes the step-by-step process to build both electrical and magnetic stimulators used to stimulate biological tissues. The protocol includes a guideline to simulate computationally electric and magnetic fields and manufacture of stimulator devices.

ABSTRACT:
Electric fields (EFs) and magnetic fields (MFs) have been widely used by tissue engineering to improve cell dynamics such as proliferation, migration, differentiation, morphology, and molecular synthesis. However, variables such stimuli strength and stimulation times need to be considered when stimulating either cells, tissues or scaffolds. Given that EFs and MFs vary according to cellular response, it remains unclear how to build devices that generate adequate biophysical stimuli to stimulate biological samples. In fact, there is a lack of evidence regarding the calculation and distribution when biophysical stimuli are applied. This protocol is focused on the design and manufacture of devices to generate EFs and MFs and implementation of a

computational methodology to predict biophysical stimuli distribution inside and outside of biological samples. The EF device was composed of two parallel stainless-steel electrodes located at the top and bottom of biological cultures. Electrodes were connected to an oscillator to generate voltages (50, 100, 150 and 200 Vp-p) at 60 kHz. The MF device was composed of a coil, which was energized with a transformer to generate a current (1 A) and voltage (6 V) at 60 Hz. A polymethyl methacrylate support was built to locate the biological cultures in the middle of the coil. The computational simulation elucidated the homogeneous distribution of EFs and MFs inside and outside of biological tissues. This computational model is a promising tool that can modify parameters such as voltages, frequencies, tissue morphologies, well plate types, electrodes and coil size to estimate the EFs and MFs to achieve a cellular response.

INTRODUCTION:

EFs and MFs have been shown to modify cell dynamics, stimulating proliferation and increasing synthesis of the main molecules associated with the extracellular matrix of tissues[1]. These biophysical stimuli can be applied in different ways by using specific settings and devices. Regarding the devices to generate EFs, direct coupling stimulators use electrodes that are in contact with biological samples in vitro or implanted directly into tissues of patients and animals in vivo[2]; however, there are still limitations and deficiencies that include insufficient biocompatibility by the electrodes in contact, changes in the pH and molecular oxygen levels[1]. On the contrary, indirect coupling devices generate EFs between two electrodes, which are placed in parallel to biological samples[3], allowing a non-invasive alternative technique to stimulate biological samples and avoid direct contact between tissues and electrodes. This type of device can be extrapolated to future clinical applications to perform procedures with minimal invasion to the patient. In relation to devices that generate MFs, inductive coupling stimulators create a time-varying electric current, which flows through a coil that is located around cell cultures[4,5]. Finally, there are combined devices, which use EFs and static MFs to generate transient electromagnetic fields[1]. Given that there are different configurations to stimulate biological samples, it is necessary to consider variables such as tension and frequency when biophysical stimuli are applied. Voltage is an important variable, since it influences the behavior of biological tissues; for instance, it has been shown that cell migration, orientation and gene expression depend on the amplitude of applied voltage[3,6-10]. Frequency plays an important role in biophysical stimulation, as it has been evidenced that these occur naturally in vivo. It has been demonstrated that high and low frequencies have beneficial effects on cells; especially, in cell membrane voltage-gated calcium channels or endoplasmic reticulum, which trigger different signaling-pathways at intracellular level[1,7,11].

According to the abovementioned, a device for generating EFs consists of a voltage generator connected to two parallel capacitors[12]. This device was implemented by Armstrong et al. to stimulate both the proliferative rate and the molecular synthesis of chondrocytes[13]. An adaptation of this device was performed by Brighton et al. who modified cell culture well-plates by drilling their top and bottom lids. Holes were filled by cover slides, where the bottom glasses were used to culture biological tissues. Electrodes were placed on each cover slide to generate EFs[14]. This device was used to electrically stimulate chondrocytes, osteoblasts and cartilage explants, showing an increase in cell proliferation[14-16] and molecular synthesis[3,17]. The device

designed by Hartig et al. consisted of a wave generator and a voltage amplifier, which were connected to parallel capacitors. Electrodes were made of high-quality stainless-steel located in an insulating case. The device was used to stimulate osteoblasts, showing a significant increase in proliferation and protein secretion[18]. The device used by Kim et al. consisted of a biphasic current stimulator chip, which was built using a manufacturing process of complementary semiconductors of high-voltage metal oxide. A culture well-plate was designed to culture cells over a conductive surface with electrical stimulation. Electrodes were coated in gold over silicon plates[19]. This device was used to stimulate osteoblasts, showing an increase in the proliferation and the synthesis of the vascular endothelial growth factor[19], and stimulating the production of alkaline phosphatase activity, calcium deposition and bone morphogenic proteins[20]. Similarly, this device was used to stimulate the proliferative rate and expression of vascular endothelial growth factor of human bone marrow mesenchymal stem cells[21]. The device designed by Nakasuji et al. was composed of a voltage generator connected to platinum plates. Electrodes were built to measure the electric potential at 24 different points. This device was used to stimulate chondrocytes, showing that EFs did not alter cell morphology and increased proliferation and molecular synthesis[22]. The device used by Au et al. consisted of a glass chamber equipped with two carbon rods connected to a cardiac stimulator with platinum wires. This stimulator was used to stimulate cardiomyocytes and fibroblasts, improving cell elongation and fibroblast alignment[23].

Different MF devices have been manufactured based on Helmholtz coils to stimulate several types of biological samples. For instance, Helmholtz coils have been used to stimulate proliferation and molecular synthesis of chondrocytes[24,25], enhance proteoglycan synthesis of articular cartilage explants[26], improve gene upregulation related to bone formation of osteoblast-like cells[27], and increase proliferation and molecular expression of endothelial cells[28]. Helmholtz coils generate MFs throughout two coils located one in front the other. The coils must be placed with a distance equal to the radius of the coils to ensure a homogeneous MF. The disadvantage of using Helmholtz coils lies in the coil dimensions, because they need to be big enough to generate the required MF intensity. Additionally, the distance between coils must be adequate to ensure a homogeneous distribution of MFs around biological tissues. To avoid issues caused by Helmholtz coils, different studies have been focused on solenoid coils manufacturing. Solenoid coils are based on a tube, which is wound with copper wire to generate MFs. Copper wire inputs can be connected directly to the outlet or a power supply to energize the coil and create MFs in the center of the solenoid. The more turns the coil has, the greater the MF generated. The MF magnitude also depends on the voltage and current applied to energize the coil[29]. Solenoid coils have been used to stimulate magnetically different kind of cells such as HeLa, HEK293 and MCF7[30] or mesenchymal stem cells[31].

Devices used by different authors have not considered either the adequate size of electrodes or correct length of the coil to homogeneously distribute both EFs and MFs. Furthermore, devices generate fixed voltages and frequencies, limiting their use to stimulate specific biological tissues. For this reason, in this protocol a computational simulation guideline is performed to simulate both capacitive systems and coils to ensure homogeneous distribution of EFs and MFs over biological samples, avoiding the edge effect. Additionally, it is shown that the design of electronic

circuits generate voltages and frequency between the electrodes and the coil, creating EFs and MFs that will overcome limitations caused by impedance of cell culture well-plates and air. These modifications will allow the creation of non-invasive and adaptive bioreactors to stimulate any biological tissue.

PROTOCOL:

1. Simulation of EFs and MFs

NOTE: Simulation of EFs and MFs was performed in COMSOL Multiphysics.

1.1 Select an axisymmetric 2D configuration to represent both domains electric and magnetic.

1.2 In the physic configuration, select either the **Electric Current** interface to compute EFs in parallel electrodes or the **Magnetic Field** interface to compute MFs around coils.

1.3 In the study configuration, select **Frequency Domain** to compute the response of a linear or linearized model subjected to harmonic excitation for one or several frequencies.

1.4 Once inside the interface to start building the model, follow the next steps according to the model of the interest.

1.4.1 Building a model for EFs

1.4.1.1 Create geometries. In the **Model Builder**, select **Geometry**. Then, locate the **Units** section and choose **mm**. On the **Geometry Toolbar**, select **Rectangle** and type the dimensions of each component in the **Size** and **Shape** box of the **Rectangle Window** settings**.** The geometry is composed by air, two parallel electrodes, a culture well-plate, culture media and a biological sample, which in this case is represented by a scaffold of hyaluronic acid – gelatin hydrogel (see dimensions of each element in **Table 1**). Once all geometries are built, click **Build All Objects**.

1.4.1.2 Create selections. On the **Definitions Toolbar**, click **Explicit** to create a selection for the metal domain. Select the geometries that represent the electrodes. After, right-click on **Explicit 1** to rename it. Type *Metal* in the new label text field.

1.4.1.2.1 On the other hand, on the **Definitions Toolbar**, click **Complement**. Locate the **Input Entities** section in the **Complement Settings** window. Then, under **Selections** to invert, click **Add** and select *Metal* in the Selections to invert list from the **Add dialog** box. Thereafter, right-click in **Complement 1** to rename it. Type *Model domain* in the new label text field.

1.4.1.3 Create boundaries. Click **Explicit** on the **Definitions** Toolbar. After, locate the **Input Entities** section in the **Settings** window for **Explicit** and from the **Geometric** entity level list,

choose **Boundary**. Here, select all boundaries for the bottom electrode. Right-click **Explicit 2** to rename it. Type *Ground boundaries* in the new label text field. Repeat these steps but selecting all boundaries for the upper electrode. Thereafter, right-click **Explicit 3** to rename it. Type *Terminal boundaries* in the new label text field.

1.4.1.4 Add electric currents. In the **Model Builder** window, under **Component 1** click **Electric Currents (ec)**. Then, locate the **Domain Selection** section in the **Electric Currents Settings** window. From the **Selection** list, choose *Model domain*. On the **Physics Toolbar**, click **Boundaries** and choose **Ground**. After, locate the **Boundary Selection** section in the **Ground Settings** window and choose *Ground boundaries* from the **Selection** list.

1.4.1.4.1 Thereafter, click **Boundaries** and choose **Terminal** on the **Physics Toolbar**. Finally, locate the **Boundary Selection** section in the **Terminal Settings** window and choose *Terminal boundaries* from the **Selection** list; here, locate the **Terminal** section and choose **Voltage** from the **Terminal** list and type 100 V.

1.4.1.5 Add materials. Click **Add Material** on the **Home Toolbar** to open the **Add Material** window. Search air and stainless-steel and add them to the **Model Builder** window. Then, click **Blank Material** on the **Home Toolbar** and add three new blank materials for culture media, scaffold (hydrogel) and polystyrene (culture well-plate).

1.4.1.6 Select a blank material to assign the dielectric properties. Locate the **Material Properties** list in the **Material** settings window and select relative permittivity and electric conductivity from the **Basic Properties** option list. The dielectric properties for culture media, hydrogel and culture well-plate are in **Table 2**. Repeat this procedure for all blank materials.

1.4.1.7 Assign each material to the geometries previously built. Select the air material form the **Model Builder** window; then, select the domains that correspond to air from the **Graphic** window. Repeat this step for all materials created. Make sure that each domain corresponds to the correct material. To make sure that all materials are correctly assigned, click on each material from the **Model Builder** window and observe whether the domains are highlighted in blue within the **Graphic** window.

1.4.1.8 Build mesh. Right-click **Mesh 1** in the **Model Builder** window and select **Free Triangular**. Repeat this step by selecting **Size**. In the **Mesh Setting** window select **Mesh Controlled** by the **User** from the **Sequence Type** list. Then, expand the **Mesh** options in the **Model Builder** window and click **Size**.

1.4.1.9 Locate **Element Size Parameters** in the **Size Setting** window and type 1 mm for maximum element size, 0.002 mm for minimum element size, 1.1 for maximum item growth rate, 0.2 for curvature factor and 1 for resolution of narrow regions. Then, expand the **Mesh** options in the **Model Builder** window and click **Free Triangular 1**. Here, select all domains to be meshed. Finally, click **Build All** in the **Mesh Setting** window.

1.4.1.10 Create study. Click **Study 1** in the **Model Builder** window. Then, locate the **Study Settings** section in the **Study Settings** window and clear the **Generate default plots** check box. Expand the **Study 1** node in the **Model Builder** window and click **Step 1: Frequency Domain**. Finally, locate the **Study Settings** section in the **Frequency Domain Settings** window and type 60 kHz in the **Frequencies** text field.

1.4.1.11 Calculate study. Click **Show Default Solver** on the **Study** toolbar. Then, expand the **Study 1 Solver Configurations** node in the **Model Builder** window. Expand the **Solution 1 (sol1)** node in the **Model Builder** window; thereafter, click **Stationary Solver 1** in the **Stationary Solver Settings** window and locate the **General** section and type 1e-6 in the **Relative Tolerance** text field. Finally, click **Compute** on the **Study Toolbar**.

1.4.1.12 Plot results. Select **Results** section on the **Home** toolbar and add **2D Plot Group**. Then, right-click **2D Plot Group 1** in the **Model Builder** window and choose **Surface**. Then, locate the **Data** section in the **Surface Settings** window and select **Precursor**. After, locate the **Expression** section in the **Surface Settings** window; here, click in the plus (+) symbol to open a new window and locate the follow route from the selection list (**Model - Component 1 – Electric Currents – Electric**). Here, select **ec.normE – EF Norm**. Finally, click on **Graphic** in the **Surface Settings** window to plot the results.

1.4.2 Building a model for MFs

1.4.2.1 Create geometries. In the **Model Builder**, select **Geometry**; then, locate the **Units** section and choose mm. On the **Geometry Toolbar** select **Rectangle** and type the dimensions of each component in the Size and Shape box of the **Rectangle Window** Settings**.** The geometry is composed by air and cooper (see dimensions of each element in **Table 1**). Once all geometries are built, click **Build All Objects**.

1.4.2.2 Add materials. Click **Add Material** on the **Home Toolbar** to open the **Add Material** window. Search air and copper and add them to the **Model Builder** window. The dielectric properties for copper are in **Table 2**.

1.4.2.3 Create boundaries. Click **Magnetics Field** on the **Model Builder** window. Here, locate **Equation** list on the **Magnetic Fields Settings** window and choose **Frequency Domain** equation from the **Equation Form** list. In **Frequency** list choose **From solver**. After, locate **Ampere's Law** on the **Magnetic Field** list in the **Model Builder** window. In the type 293.15[K] in **Temperature**, 1[atm] in **Absolute Pressure** from the **Inputs Mode**l list. Then, choose **Solid** from the **Material** type list in the Ampere's Law Settings window. Make sure that Electric conductivity, Relative permittivity and Relative Permeability correspond to the From material in the list.

1.4.2.4 Locate **Axial Symmetry** on the **Magnetic Field** list in the **Model Builder** window. Make sure that the axial symmetry line is highlighted in both **Boundary Selection** list and **Graphic** window. Then, locate **Magnetic Isolation** on the **Magnetic Field** list in the **Model Builder** window. Make sure that boundaries from the geometry are highlighted in both **Boundary Selection** list

and **Graphic** window.

1.4.2.5 Locate **Initial Values** on the **Magnetic Field** list in the **Model Builder** window. Select geometries previously built and include them in the Domain Selection from the **Initial Values Settings** window.

1.4.2.6 Introduce coil features. Locate **Multiple Coil** on the **Magnetic Field** list in the **Model Builder** window. Here, selects the geometry that represents the coil and include them in the **Domain Selection** from the **Multiple Coil Settings** window.

1.4.2.7 Locate the **Multiple Coil** list on the **Multiple Coil Setting** window; here, locate Coil excitation list and select **Current**; thereafter, type 1[A] in the Coil current list, 450 in the Number of turns and 6e7[S/m] in the Coil conductivity.

1.4.2.8 Locate the **Coil** wire cross-sectional area and choose North American cable diameter (Brown & Sharpe) from the list and type 18 in the AWG option. Make sure that Relative permittivity and Relative Permeability correspond to From material in the list.

1.4.2.9 Build mesh. In the **Mesh Setting** window select **Mesh Controlled** by the physics from the **Sequence Type** list. After, locate **Element Size Parameters** in the **Mesh Setting** window and select Extremely fine. Finally, select all domains to be meshed and click **Build All** in the Mesh Setting window.

1.4.2.10 Create study. Click **Study 1** in the **Model Builder** window. Then, locate the **Study Settings** section in the **Study Settings** window and clear the **Generate** default plots check box. Expand the **Study 1** node in the **Model Builder** window and click **Step 2: Frequency Domain**. Finally, locate the **Study Settings** section in the **Frequency Domain Settings** window and type 60 Hz in the Frequencies text field.

1.4.2.11 Calculate study. Click **Show Default Solver** on the **Study** toolbar. Then, expand the **Study 1 Solver Configurations** node in the **Model Builder** window. Expand the **Solution 1 (sol1)** node in the **Model Builder** window; thereafter, click **Stationary Solver 1** in the **Stationary Solver Settings** window and locate the **General** section and type 1e-6 in the **Relative tolerance** text field. Finally, click **Compute** on the **Study Toolbar**.

1.4.2.12 Plot results. Select **Results** section on the **Home** toolbar and add **2D Plot Group**. Then, right-click **2D Plot Group 1** in the **Model Builder** window and choose **Surface**. Then, locate the **Data** section in the **Surface Settings** window and select **Precursor**.

1.4.2.13 Locate the **Expression** section in the **Surface Settings** window. Here, click in the plus (+) symbol to open a new window and locate the follow route from the selection list (**Model - Component 1 – Magnetic Field – Magnetic**). Here, select **mf.normB – Magnetic flux density Norm**. Finally, click on **Graphic** in the **Surface Settings** window to plot the results.

2. Design and manufacturing of the electrical and magnetic stimulation devices

2.1 The electrical stimulator device

NOTE: It is composed by a circuit based on the Wien Bridge Oscillator and two parallel stainless-steel electrodes. The circuit is a RC oscillator of phase shift, which uses a positive and negative feedback. The Wien Bridge Oscillator is composed by a lead-lag network, which divides the input voltage by the combination of two arms of the bridge: a resistor R_5 with a capacitor C_2 in series, and a resistor R_6 with a capacitor C_3 in parallel (**Figure 1A**). These components modulate the frequency of the oscillator. To build the electrical stimulator device follow the next steps:

2.1.1 Calculate the frequency using the resonant frequency equation (1).

$$f = \frac{1}{2\pi RC} \qquad (1)$$

Where $R = R_5 = R_6$ are resistors and $C = C_2 = C_3$ are capacitors. Both R and C are placed in the two arms of the bridge (**Figure 1A**). Use $R_5 = R_6 = 2.6\ \text{k}\Omega$ and $C_2 = C_3 = 1\ \text{nF}$ to obtain a frequency of 60 kHz. Resistors and capacitors may be calculated if a different frequency is required.

2.1.2 Design the circuit in such a way that voltage gain of the amplifier automatically compensates the amplitude changes of the output signal. In **Figure 1A** it is possible to observe the scheme of the circuit, while in **Table of Materials** section are listed the electronic components to build the circuit.

2.1.3 Calculate the combination of resistors to generate the four output voltages. As shown in **Figure 1A**, use a combination of resistors R_{11}, R_{12}, R_{13} and R_{14} (equivalent resistance of 154 Ω) to generate a voltage of 50 Vp-p; resistors R_{17}, R_{18} and R_{19} in series (equivalent resistance of 47,3 Ω) to obtain a voltage of 100 Vp-p; resistors R_9 and R_{10} in series (equivalent resistance of 25,3 Ω) to generate a voltage of 150 Vp-p; and a combination of resistors R_{15} and R_{16} (equivalent resistance of 16,8 Ω) to obtain a voltage of 200 Vp-p.

2.1.4 Use a transistor (TIP 31C) and a ferrite core transformer to implement a signal amplification stage. A toroidal ferrite core was used to wind an AWG 24 copper wire, completing a relation 1:200. Use two capacitors (C_4 and C_5) of 100 nF in parallel before the transformer to rectify the signal (**Figure 1A**).

2.1.5 Prepare the PCB using a third-party PCB manufacturing service. The schematic diagram of the circuit is provided in **Figure 1**. Place all components on the PCB with antistatic tweezers. Use tin solder and soldering iron to solder all components.

2.1.6 Manufacture a plastic case with input connectors to protect the circuit. Implement three

input connectors to energize the circuit (12 V, -12 V and ground). Use two input connectors to connect the electrodes. Include three switches to change the resistors combination to obtain the four output voltages. Assemble the electronic circuit into the plastic case (**Figure 1B**).

2.1.7 Manufacture two parallel stainless-steel electrodes (200 x 400 x 2 mm) and solder input connectors to each edge. The electrodes are located over Teflon or acrylic supports to eliminate any contact with the metal surface of the incubator (**Figure 1C**).

2.1.8 Use an autoclave at 394.15 K (121 °C) for 30 minutes to sterilize the electrodes and use ultraviolet over night to sterilize the wires that are in contact with the incubator.

2.1.9 Test the electrical stimulation device. Adjust the power supply in series to generate an output voltage of +12 V and -12 V between the ground and positive and negative terminals. Verify the output voltage of the power supply with a multimeter. Connect each output of the power supply in the correct input of the electrical stimulator (+12 V, -12 V and ground). Connect each electrode in the correct input connector of the electrical stimulator. The polarity is not important, as we are working on AC current. Place a culture well-plate between of the electrodes and verify the output signal with an oscilloscope. Adjust the switches of the electrical stimulator to generate the four output voltages (50, 100, 150 and 200 Vp-p).

2.1.10 Safety recommendations. To avoid any issue when transferring or removing the electrodes from the incubator make sure that cables are not tangled. Disconnect cables from the oscillator before removing the electrodes from the incubator. Never place the electrodes without the acrylic or Teflon supports.

2.2 The magnetic stimulator device

2.2.1 Estimate the number of turns to guarantee a homogeneous MF inside the coil using the equation (2), that describes the MF inside a solenoid coil.

$$B_{int} = \frac{\mu_0 NI}{h} \quad (2)$$

where μ_0 is the magnetic permeability of the vacuum ($4\pi x 10^{-7}$), N is the number of turns of the copper wire, I is the current, and h, which should be greater than its diameter, is the length of the solenoid coil.

2.2.2 Determine the number of turns by choosing a length (h) of 250 mm, current of 1 A and a $B_{int} = 2mT$.

2.2.3 Manufacture the coil. Build a polyvinyl chloride (PVC) tube with a length of 250 mm and a diameter of 84 mm to wind an AWG 18 copper wire completing 450 turns (**Figure 2A**). Dimensions were chosen based on the available space inside the incubator.

2.2.4 Manufacture a cell culture well-plate support. Build a polymethyl methacrylate (PMMA) support to ensure that well-plates of 35 mm were always located in the middle of the coil where MFs are homogeneous (**Figure 2A**).

2.2.5 Manufacture a transformer to increase the current of the circuit. Build a transformer with an output of 1 A - 6 V AC to reach a maximum MF of 2 mT. The input voltage of the transformer was 110 V AC at 60 Hz. These parameters correspond to the output voltage and frequency of a South America outlet.

2.2.6 Connect the circuit. The transformer is connected directly to the outlet. Use a variable resistor (rheostat) to vary the current and generate MFs from 1 to 2 mT. Connect a fuse to protect the circuit (**Figure 2B**).

2.2.7 Use ultraviolet over night to sterilize the wires that are in contact with the incubator. Wrap the coil with transparent stretch film and use ethanol to sterilize the coil.

2.2.8 Test the MF device. Use a teslameter to measure the MF magnitude inside the coil. The teslameter probe was located in the center of the coil, allowing the measurement of MFs and currents simultaneously.

2.2.9 Vary the MF magnitude. Use a rheostat to modify the resistance of the circuit (**Figure 2B**). A resistance value of 0.7 Ω was used to generate MFs of 1 mT.

2.2.10 Safety recommendations. To avoid any issue when transferring or removing the solenoid from the incubator make sure that cables are not tangled. Disconnect cables from the transformer before removing the solenoid from the incubator. Never place the solenoid without the PMMA support. Firmly grasp both PMMA support from the base and the solenoid when transferring or removing from the incubator.

REPRESENTATIVE RESULTS:

Computational simulation

Distributions of EFs and MFs are shown in **Figure 3**. On the one hand, it was possible to observe the homogeneous distribution of EFs in the capacitive system (**Figure 3A**). The EF was plotted to observe in detail the magnitude of the field inside the biological sample (**Figure 3B**). This simulation was useful to parametrize the size of the electrodes and manufacture them to avoid the edge effect. On the other hand, it was possible to observe the homogeneous distribution of MFs generated by the solenoid coil (**Figure 3C**). The MF was plotted to observe in detail the magnitude of the field inside the coil (**Figure 3D**). This simulation was important measure the distance where the MF is the same and build the PMMA support. This support ensures a homogeneous distribution of the MF not only in the center of the coil, but also in the biological samples to be stimulated.

Signals generated by electrical and magnetic stimulators

Output signals generated by electrical stimulator are shown in **Figure 4**. It is relevant to highlight that signals captured by the oscilloscope were directly taken in the electrodes, as whether the measurement is taken directly to the output cables, the voltages will be higher (**Figure 4A**). This voltage variation is given by the capacitance of electrodes. The output voltage oscillates in a range of ± 5V at 60 kHz; for instance, the output signals were 54.9 Vp-p (**Figure 4B**), 113 Vp-p (**Figure 4C**), 153 Vp-p (**Figure 4D**) and 204 Vp-p (**Figure 4E**) for 50, 100, 150 and 200 Vp-p, respectively.

The output signal generated by the magnetic stimulator is shown in **Figure 5**. The signal captured by the oscilloscope were directly taken in the output cables of the coil (**Figure 5A**). The output voltage oscillates in range of ± 15V p-p at 60 Hz (**Figure 5B**).

Figure 1. Electrical stimulation device. **A)** Circuit that generates tensions of 50, 100, 150 and 200 Vp-p at 60 kHz sine wave-form. **B)** Printed circuit board within the case. **C)** Electrodes inside the incubator.

Figure 2. Magnetic stimulation device. **A**) Schematic representation of the magnetic stimulator device and the PMMA support. **B**) Circuit to generate the MFs.

Figure 3. Computational simulation of EFs and MFs. A) Distribution of EFs inside and outside the capacitive system. **B)** Distribution of EFs within the hydrogel, the region of interest is indicated in a red detail. **C)** Distribution of MFs inside and outside the coil. **D)** Distribution of MFs in the center of the coil, the region of interest is indicated in a red detail.

Figure 4. Sinusoidal signal generated by electrical stimulator. A) Signal verification generated by the electrical stimulator. **B)** Signal at 50 Vp-p. **C)** Signal at 100 Vp-p. **D)** Signal at 150 Vp-p. **E)** Signal at 200 Vp-p. All measurements oscillate in a range of ± 5V at 60 kHz.

Figure 5. Sinusoidal signal generated by the magnetic stimulator. A) Signal verification generated by the magnetic stimulator. **B)** Signal at 15 Vp-p at 60 Hz.

Table 1. Dimension of geometries that compose electric and magnetic systems.

Table 2. Dielectric properties of elements that compose electric and magnetic systems.

DISCUSSION:

Treatments used to heal different pathologies that affect human tissues are pharmacological therapies[32] or surgical interventions[33], which seek to relieve pain locally or replace affected tissues with explants or transplants. Recently, autologous cell therapy has been proposed as an alternative therapy to treat injured tissues, where cells are isolated from patient and expanded, through in vitro techniques, to be implanted at the site of the injury[34]. Given that autologous cell therapy has demonstrated to have direct influence over tissue recovery, different strategies has been developed to increase the effectiveness of this technique. For instance, biophysical stimuli have been used as a non-invasive alternative therapy to stimulate several types of biological

samples, modulating cell functionality by improving cell proliferation and molecular synthesis[35,36]. Among the most used biophysical stimuli, electrostimulation and magnetotherapy have been widely applied to stimulate cells, tissue explants and scaffolds. It has been evidenced that electrostimulation reduces pain and increases healing processes of several tissues[37]. Regarding the magnetotherapy, it has been described that this stimulus improves integration of implants with host tissues, accelerates healing processes, relieves pain locally and increases scar strength[8,38].

Considering the mentioned above, the combination of biomaterials, cell culture and external biophysical stimuli such as EFs and MFs, at in vitro level, has been introduced in tissue engineering as an alternative therapeutic technique to heal injured tissues[8,39]. However, finding a bioreactor that helps to stimulate different tissues, whether healthy or affected by traumatic pathologies, is a challenge. In this context, the present protocol aims to develop both electrical and magnetic stimulators. Currently, there are two possible schemes for applying EFs. The first method consists of generating EFs through direct coupling systems, which are used to evaluate cell migration and orientation[40-42]. However, there are limitations such as alterations in biocompatibility of the cell culture medium by electrodes in contact, possible changes in pH and molecular oxygen levels[1]. Additionally, direct coupled stimulation cannot amplify high-frequency signals. The output tends to vary with time, generating supply voltage changes. It has little temperature stability, due to this its operating points change and at low frequencies the capacitor fails and acts as an open circuit[43]. Considering these limitations, the second method was implemented, where external parallel electrodes were used. This indirect coupling system method has evidenced an increase in cell proliferation and molecular synthesis[3,7,17,22,44,45]; however, the devices developed by different authors have not considered the size of electrodes to distribute homogeneously EFs. For instance, devices generate fixed voltages and frequencies, limiting their use in stimulating specific cells and tissues. Accordingly, in this study the size of the electrodes was modelled to ensure a homogeneous distribution of EFs over biological tissues. In addition, a circuit was designed to generate a frequency and high voltages between electrodes, creating different EFs that overcome the limitations caused by the impedance of cell culture well-plates and air.

Solenoid coils are versatile devices that can be used to stimulate biological samples within the incubator, allowing that atmospheric conditions remain stable without affecting physiological features of biological samples. This advantage elucidates that solenoid coils are feasible alternatives more than Helmholtz coils, as these need to be bigger in size, preventing stimulation inside incubators[46]. Stimulation of biological samples outside the incubator can lead in several issues such as cell culture contamination, cell stress, pH changes of culture media, among others. Given that different stimulator devices have been developed to stimulate several cell types and tissues[24-27], it is relevant to build devices where MF intensities can be varied to stimulate a wide range of biological samples[29,30]. Accordingly, in this protocol the magnetic stimulator is connected to a rheostat, which can vary the current that flows through the solenoid by modifying their resistance and current, parameters that are directly related to the generation of MFs. Another important feature to consider at the moment of building magnetic devices is the distribution of MFs. Here, a computational simulation was used to simulate the MF distribution

inside the solenoid coil. This simulation allowed to calculate the number of turns of the copper wire and the length of the coil to generate homogeneous MFs in the middle of the coil. The computational simulation is a useful tool to calculate the number of biological samples to be stimulated, ensuring that all samples receive the same field strength[47].

The biophysical stimulators developed in this protocol have some limitations. First, the electronic circuit designed for electrical stimulator generates four output voltages at a specific frequency. Although the circuit overcome the limitation of generating high voltages between electrodes[1], it could be improved to generate variable voltages and frequencies. The circuit can be modified to generate different frequencies just calculating either resistors or capacitors using equation (1); however, it is possible to use variable resistors to vary manually the resistor value. Similarly, a variable resistor may be use in the amplification stage of the circuit to vary the output voltage. Second, the electronic circuit of the electrical stimulator generates sinusoidal signals. It would be useful to generate different kind of signals such as square, triangular, trapezoidal and ramp, as these types of signals could be used to stimulate a wide range of cells and biological samples[48,49]. To generate different type of signals, the operational amplifier can be replaced by a monolithic function generator, which can produce high quality waveforms of high-stability and accuracy with low amplitude, and the amplification stage can be replaced by a non-inverting operational amplifier or a stage with NPN transistors. Third, even though the magnetic stimulator generates small MF magnitudes, it has been evidenced that these intensities have direct impact over dynamics of biological samples[24,28,30,38]; however, the magnetic device could be improved to generate variable MFs and frequencies to stimulate a wide range of biological tissues[29].

Overall, this protocol is a useful tool which provides a technological contribution to the scientific community that works on biophysical stimulation of biological tissues. These devices will allow researchers to use EFs and MFs to stimulate the function of healthy biological tissues or those altered by a particular pathology. Considering this in further in vivo studies, different parameters and variables such as electrodes size, number of turns of the coil, stimuli strength and stimulation times would be determined to homogeneously distribute both EFs and MFs in animals such as pigs, calves, guinea pigs or rabbits. Additionally, bioreactors designed in this protocol can be extrapolated to clinical settings to improve regenerative techniques such as autologous cell implantation. Here, bioreactors can play an important role by stimulating biological samples, at the *in vitro* level, to improve the cellular and molecular features of cells, tissues and scaffolds before being implanted in the patient.

ACKNOWLEDGMENTS:

The authors thank the financial support provided by “Fondo Nacional de Financiamiento para la Ciencia, la Tecnología, y la Innovación -Fondo Francisco José de Caldas- Minciencias” and Universidad Nacional de Colombia through the grant No. 80740-290-2020 and the support received by *Valteam Tech - Research and Innovation* for providing the equipment and technical support in the edition of the video.

DISCLOSURES:

The authors declare that they have no conflict of interest.

REFERENCES:

[1] Balint, R., Cassidy, N. J., Cartmell, S. H. Electrical Stimulation: A Novel Tool for Tissue Engineering. *Tissue Engineering Part B: Reviews*. **19** (1), 48–57 (2013).

[2] Ercan, B., Webster, T. J. The effect of biphasic electrical stimulation on osteoblast function at anodized nanotubular titanium surfaces. *Biomaterials*. **31** (13), 3684–3693 (2010).

[3] Brighton, C., Wang, W., Clark, C. The effect of electrical fields on gene and protein expression in human osteoarthritic cartilage explants. *The Journal of Bone and Joint Surgery-American Volume*. **90** (4), 833–848 (2008).

[4] Baerov, R. M., Morega, A. M., Morega, M. Analysis of magnetotherapy effects for post–traumatic recovery of limb fractures. *Revue Roumaine des Sciences Techniques– Série électrotechnique et énergétique*. **65** (1–2), 145–150 (2020).

[5] Escobar, J. F. et al. In Vitro Evaluation of the Effect of Stimulation with Magnetic Fields on Chondrocytes. *Bioelectromagnetics*. **41** (1), 41–51 (2019).

[6] Brighton, C., Wang, W., Clark, C. Up-regulation of matrix in bovine articular cartilage explants by electric fields. *Biochemical and Biophysical Research Communications*. **342** (2), 556–561 (2006).

[7] Xu, J., Wang, W., Clark, C., Brighton, C. Signal transduction in electrically stimulated articular chondrocytes involves translocation of extracellular calcium through voltage-gated channels. *Osteoarthritis and Cartilage*. **17** (3), 397–405 (2009).

[8] Xia, Y. et al. Magnetic field and nano-scaffolds with stem cells to enhance bone regeneration. *Biomaterials*. **183**, 151–170 (2018).

[9] Richter, A., Bartoš, M., Ferková, Ž. Physical Analysis of Pulse Low-Dynamic Magnetic Field Applied in Physiotherapy BT - *World Congress on Medical Physics and Biomedical Engineering 2018*. 239–245 (2019).

[10] Miyakoshi, J. Effects of static magnetic fields at the cellular level. *Progress in Biophysics and Molecular Biology*. **87**, 213–223 (2005).

[11] Zhang, K., Guo, J., Ge, Z., Zhang, J. Nanosecond Pulsed Electric Fields (nsPEFs) Regulate Phenotypes of Chondrocytes through Wnt/β-catenin Signaling Pathway. *Scientific Reports*. **4** (5836), 1–8 (2014).

[12] Brighton, C. T., Unger, A. S., Stambough, J. L. In vitro growth of bovine articular cartilage chondrocytes in various capacitively coupled electrical fields. *Journal of Orthopaedic Research*. **2** (1), 15–22 (1984).

[13] Armstrong, P. F., Brighton, C., Star, A. M. Capacitively coupled electrical stimulation of bovine growth plate chondrocytes grown in pellet form. *Journal of Orthopaedic Research*. **6** (2), 265–271 (1988).

[14] Brighton, C., Townsend, P. Increased cAMP production after short-term capacitively coupled stimulation in bovine growth plate chondrocytes. *Journal of Orthopaedic Research*. **6** (4), 552–558 (1988).

[15] Brighton, C. T., Jensen, L., Pollack, S. R., Tolin, B. S., Clark, C. Proliferative and synthetic response of bovine growth plate chondrocytes to various capacitively coupled electrical fields. *Journal of Orthopaedic Research*. **7** (5), 759–765 (1989).

[16] Brighton, C. T., Okereke, E., Pollack, S. R., Clark, C. In vitro bone-cell response to a capacitively coupled electrical field. The role of field strength, pulse pattern, and duty cycle.

615 *Clinical Orthopaedics and Related Research* (**285**), 255–262 (1992).
616 [17] Wang, W., Wang, Z. , Zhang, G., Clark, C., Brighton, C. T. Up-regulation of chondrocyte
617 matrix genes and products by electric fields. *Clinical Orthopaedics and Related Research* (**427**
618 SUPPL.), 163–173 (2004).
619 [18] Hartig, M., Joos, U., Wiesmann, H. P. Capacitively coupled electric fields accelerate
620 proliferation of osteoblast-like primary cells and increase bone extracellular matrix formation in
621 vitro. *European Biophysics Journal*. **29** (7), 499–506 (2000).
622 [19] Kim, I. S. et al. Biphasic electric current stimulates proliferation and induces VEGF
623 production in osteoblasts. *Biochimica et Biophysica Acta (BBA) - Molecular Cell Research*. **1763**
624 (9), 907–916 (2006).
625 [20] Kim, I. et al. Novel Effect of Biphasic Electric Current on In Vitro Osteogenesis and Cytokine
626 Production in Human Mesenchymal Stromal Cells. *Tissue Engineering Part A*. **15**, 2411–2422
627 (2009).
628 [21] Kim I. et al. Novel action of biphasic electric current in vitro osteogenesis of human bone
629 marrow mesenchymal stromal cells coupled with VEGF production. *Bone*. **43**, 43–44 (2008).
630 [22] Nakasuji, S., Morita, Y., Tanaka, K., Tanaka, T., Nakamachi, E. Effect of pulse electric field
631 stimulation on chondrocytes. *Asian Pacific Conference for Materials and Mechanics. 2009*
632 *Yokohama, Japan, Novemb. 13-16*. **1**, 13–16 (2009).
633 [23] Au, H. T. H., Cheng, I., Chowdhury, M. F., Radisic, M. Interactive effects of surface
634 topography and pulsatile electrical field stimulation on orientation and elongation of fibroblasts
635 and cardiomyocytes. *Biomaterials*. **28** (29), 4277–4293 (2007).
636 [24] Vanessa, N. et al. In vitro exposure of human chondrocytes to pulsed electromagnetic
637 fields. *European Journal of Histochemistry*. **51** (3), 203–211 (2007).
638 [25] Pezzetti, F. et al. Effects of pulsed electromagnetic fields on human chondrocytes: An in
639 vitro study. *Calcified Tissue International*. **65** (5), 396–401 (1999).
640 [26] De Mattei, M. et al. Effects of electromagnetic fields on proteoglycan metabolism of
641 bovine articular cartilage explants. *Connective Tissue Research*. **44** (3–4), 154–159 (2003).
642 [27] Sollazzo, V., Massari, L., Caruso, A., Mattei, M., Pezzetti, F. Effects of Low-Frequency
643 Pulsed Electromagnetic Fields on Human Osteoblast-Like Cells In Wtro. *Electromagnetobiology*.
644 **15**), 75–83 (2009).
645 [28] Martino, C. F., Perea, H., Hopfner, U., Ferguson, V. L., Wintermantel, E. Effects of weak
646 static magnetic fields on endothelial cells. *Bioelectromagnetics*. **31** (4), 296–301 (2010).
647 [29] Wada, K. et al. Design and implementation of multi-frequency magnetic field generator
648 producing sinusoidal current waveform for biological researches, in *2016 18th European*
649 *Conference on Power Electronics and Applications (EPE'16 ECCE Europe)*. **2016**), 1–8 (2016).
650 [30] Cho, H., Kim, S., Kim, K. K., Kim, K., Kim, K. Pulsed Electromagnetic Fields Stimulate Cellular
651 Proliferation in Different Types of Cells. *IEEE Transactions on Magnetics*. **52** (7), 1–4 (2016).
652 [31] Yan, J., Dong, L., Zhang, B., Qi, N. Effects of extremely low-frequency magnetic field on
653 growth and differentiation of human mesenchymal stem cells. *Electromagnetic Biology and*
654 *Medicine*. **29** (4), 165–176 (2010).
655 [32] Enoch, S., Grey, J. E., Harding, K. G. ABC of wound healing. Non-surgical and drug
656 treatments. *BMJ*. **332** (7546), 900–903 (2006).
657 [33] Bhosale, A. M., Richardson, J. B. Articular cartilage: Structure, injuries and review of
658 management. *British Medical Bulletin*. **87** (1), 77–95 (2008).

[34] Al Hamed, R., Bazarbachi, A. H., Malard, F., Harousseau, J.-L., Mohty, M. Current status of autologous stem cell transplantation for multiple myeloma. *Blood Cancer Journal*. **9** (4), 44 (2019).
[35] Massari, L. et al. Biophysical stimulation of bone and cartilage: state of the art and future perspectives. *International Orthopaedics*. **43** (3), 539–551 (2019).
[36] Naskar, S., Kumaran, V., Basu, B. Reprogramming the Stem Cell Behavior by Shear Stress and Electric Field Stimulation: Lab-on-a-Chip Based Biomicrofluidics in Regenerative Medicine. *Regenerative Engineering and Translational Medicine*. **5** (2), 99–127 (2019).
[37] Hunckler, J., de Mel, A. A current affair: electrotherapy in wound healing. *Journal of Multidisciplinary Healthcare*. **10**), 179–194 (2017).
[38] Henry, S. L., Concannon, M. J., Yee, G. J. The effect of magnetic fields on wound healing: experimental study and review of the literature. *Eplasty*. **8**, 393–399 (2008).
[39] Hiemer, B. et al. Effect of electric stimulation on human chondrocytes and mesenchymal stem cells under normoxia and hypoxia. *Molecular Medicine Reports*. **18** (2), 2133–2141 (2081).
[40] Chao, P. H. et al. Chondrocyte translocation response to direct current electric fields. *Journal of Biomechanical Engineering*. **122** (3), 261–267 (2000).
[41] Zhao, M., Bai, H., Wang, E., Forrester, J., McCaig, C. Electrical stimulation directly induces pre-angiogenic responses in vascular endothelial cells by signaling through VEGF receptors. *Journal of Cell Science*. **117** (3), 397–405 (2004).
[42] Li, X., Kolega, J. Effects of direct current electric fields on cell migration and actin filament distribution in bovine vascular endothelial cells. *Journal of Vascular Research*. **39** (5), 391–404 (2002).
[43] Singh, B., Dixit, A. Multistage amplifier and tuned amplifier. *Analog Electronics*, Boston, MA: Laxmi publications (P) LTD, 87–131 (2007).
[44] Esfandiari, E. et al. The effect of high frequency electric field on enhancement of chondrogenesis in human adipose-derived stem cells. *Iranian Journal Basic Medical Sciences*. **4** (3), 571–576 (2014).
[45] Mardani, M. et al. Induction of chondrogenic differentiation of human adipose-derived stem cells by low frequency electric field. *Advanced Biomedical Research*. **5** (97), 1–7 (2016).
[46] Karaman, O., Gümüşay, M., Demirci, E. A., Kaya, A. Comparative assessment of pulsed electromagnetic fields (PEMF) and pulsed radio frequency energy (PRFE) on an in vitro wound healing model. *International Journal of Applied Electromagnetics and Mechanics*. **57**, 427–437 (2018).
[47] Glinka, M. et al. Test chambers for cell culture in static magnetic field. *Journal of Magnetism and Magnetic Materials*. **331**, 208–215 (2013).
[48] Vacek, T. P. et al. Electrical stimulation of cardiomyocytes activates mitochondrial matrix metalloproteinase causing electrical remodeling. *Biochemical and Biophysical Research Communications*. **404** (3), 762–766 (2011).
[49] Okutsu, S. et al. Electric Pulse Stimulation Induces NMDA Glutamate Receptor mRNA in NIH3T3 Mouse Fibroblasts. *The Tohoku Journal of Experimental Medicine*. **215** (2), 181–187 (2008).

Figure 1

Click here to access/download;Figure;Figure 1.png

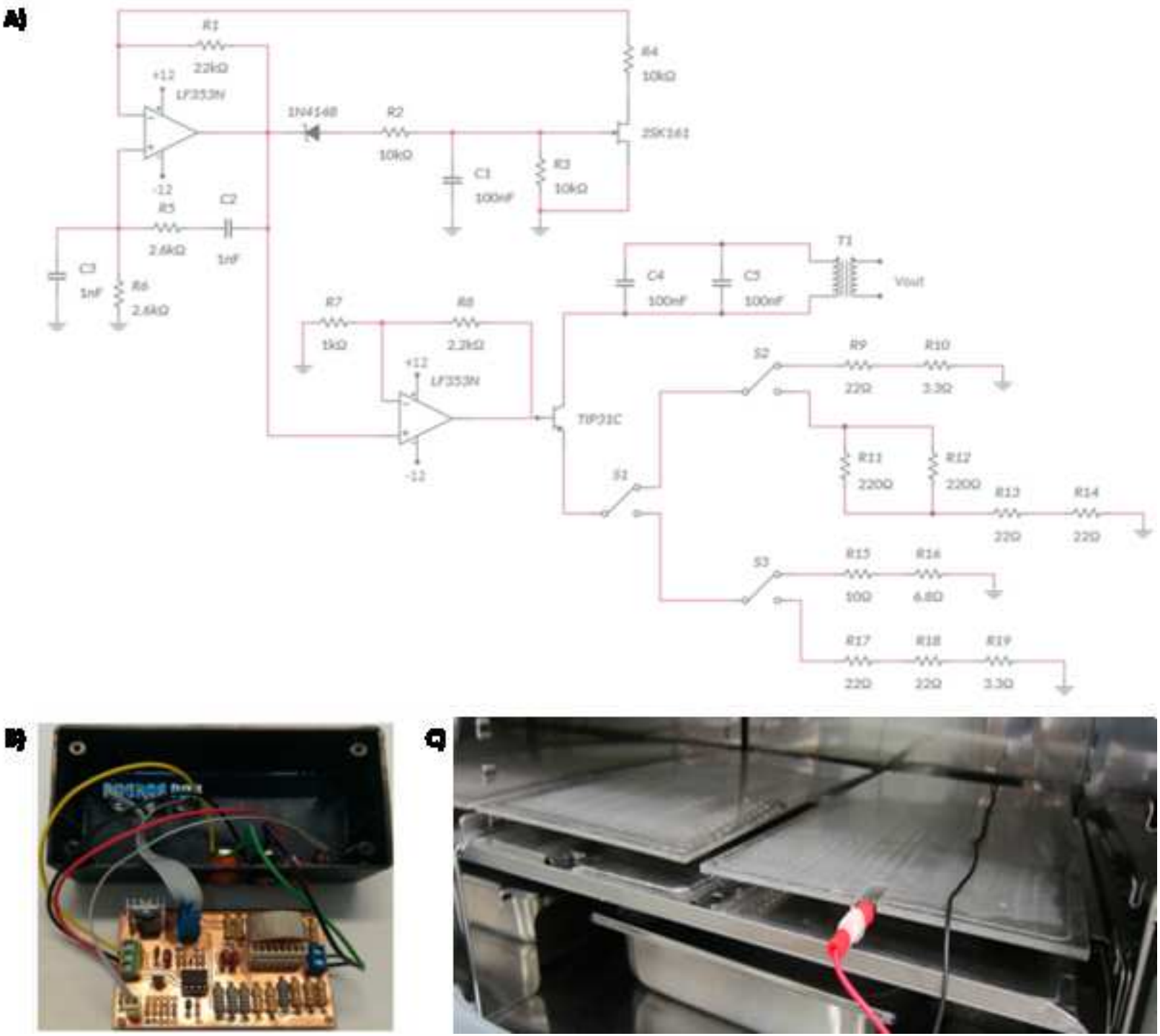

Figure 2

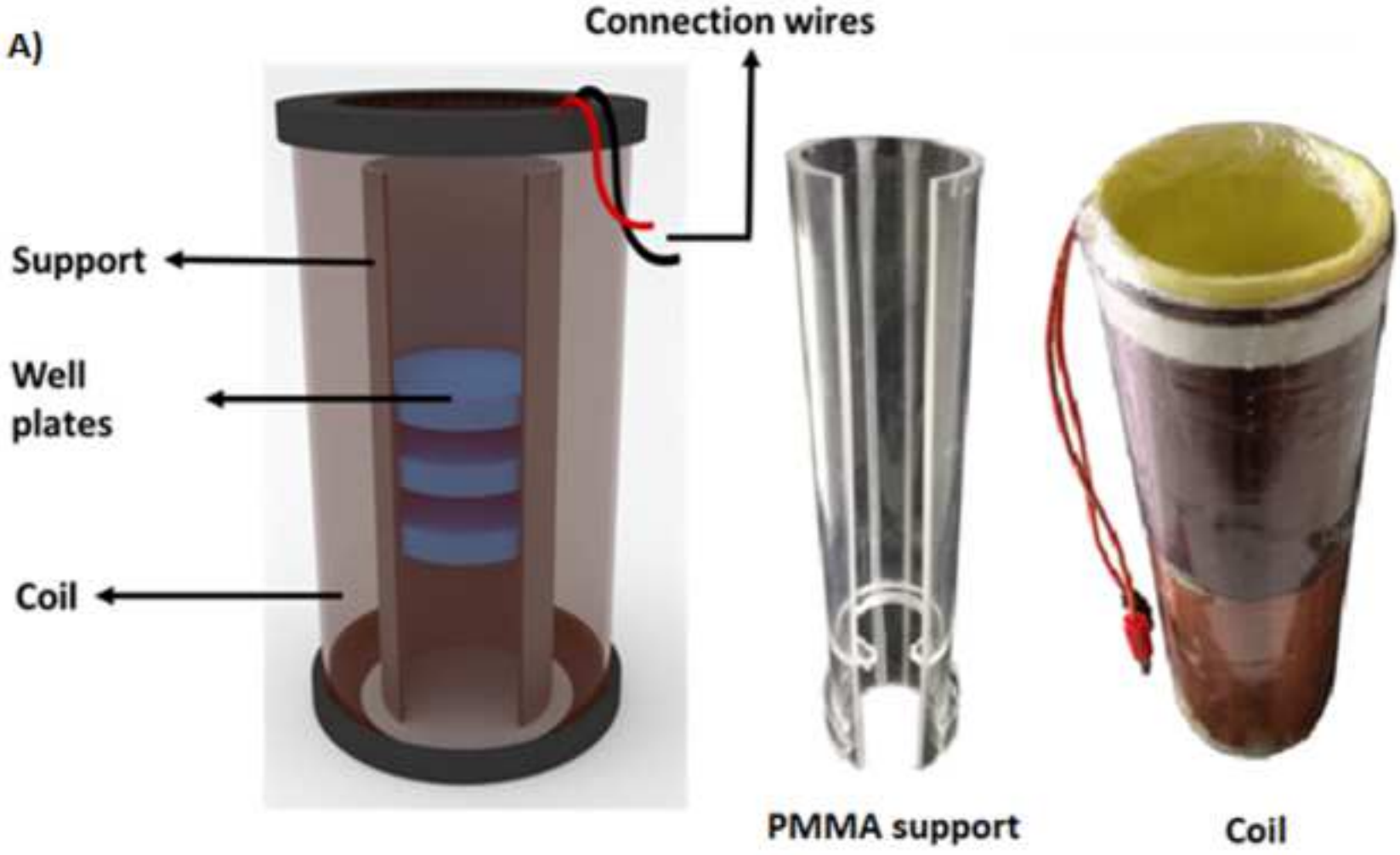

Figure 3

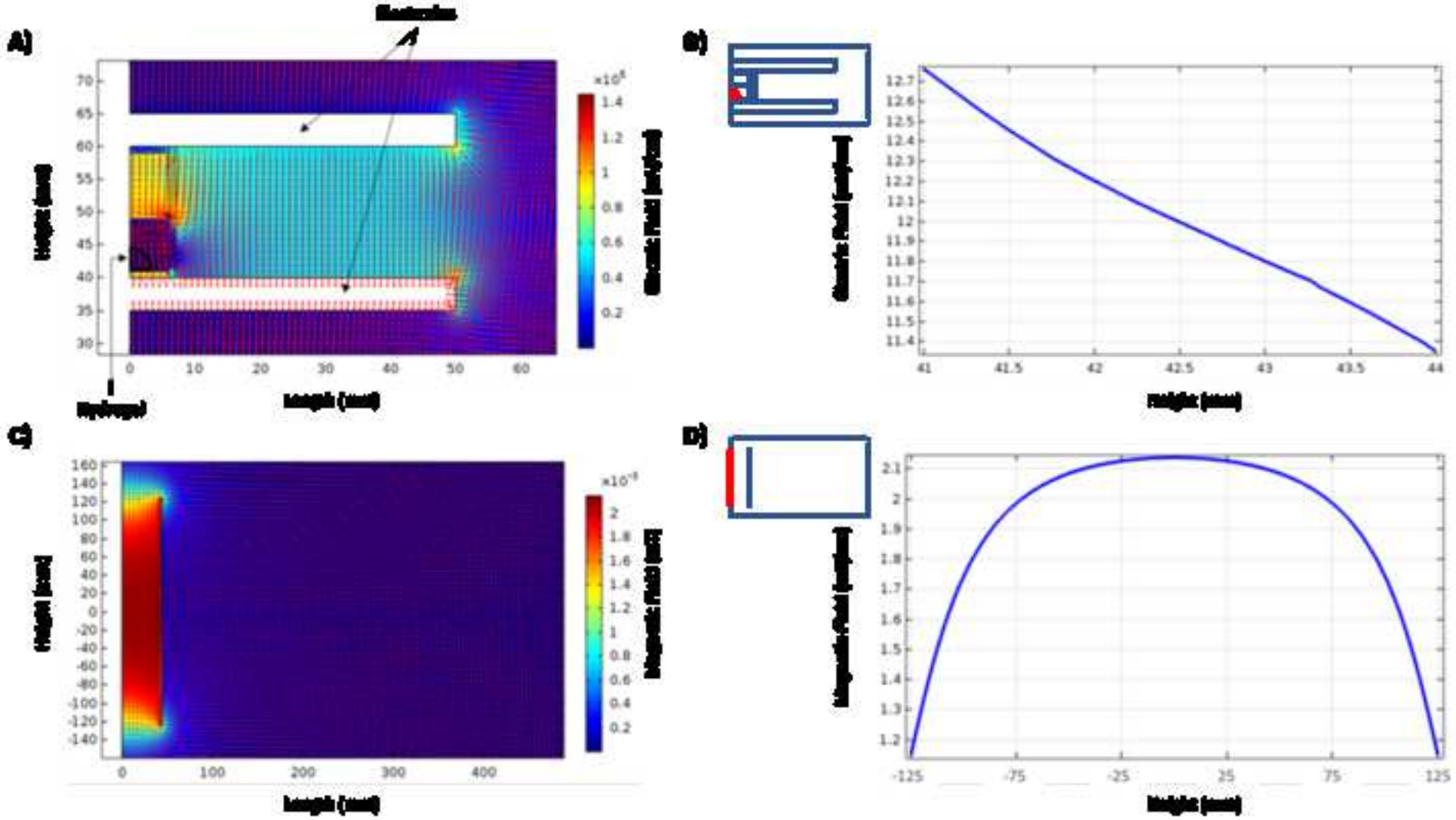

Figure 4

Click here to access/download;Figure;Figure 4.png

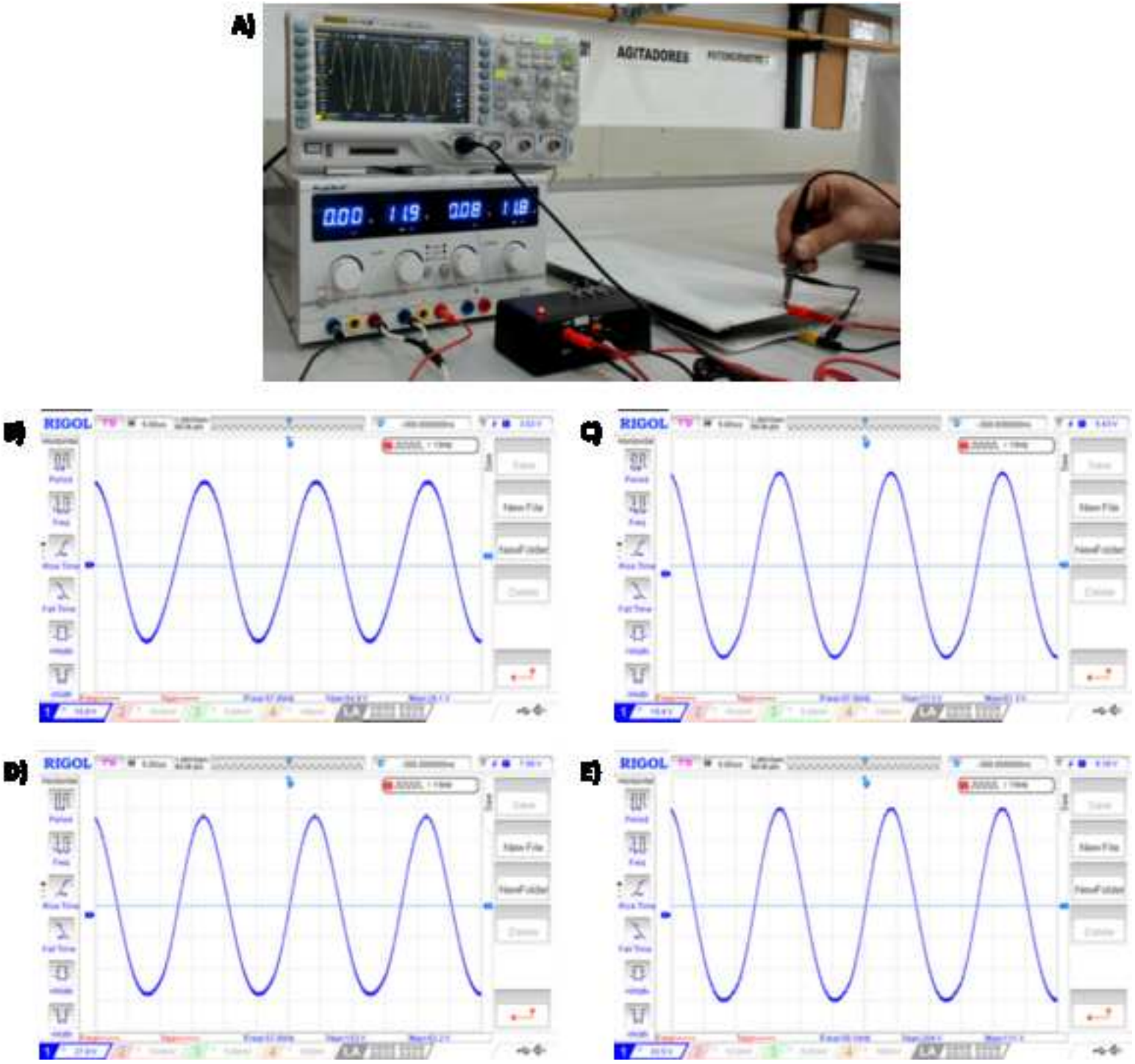

Figure 5

Click here to access/download;Figure;Figure 5.png

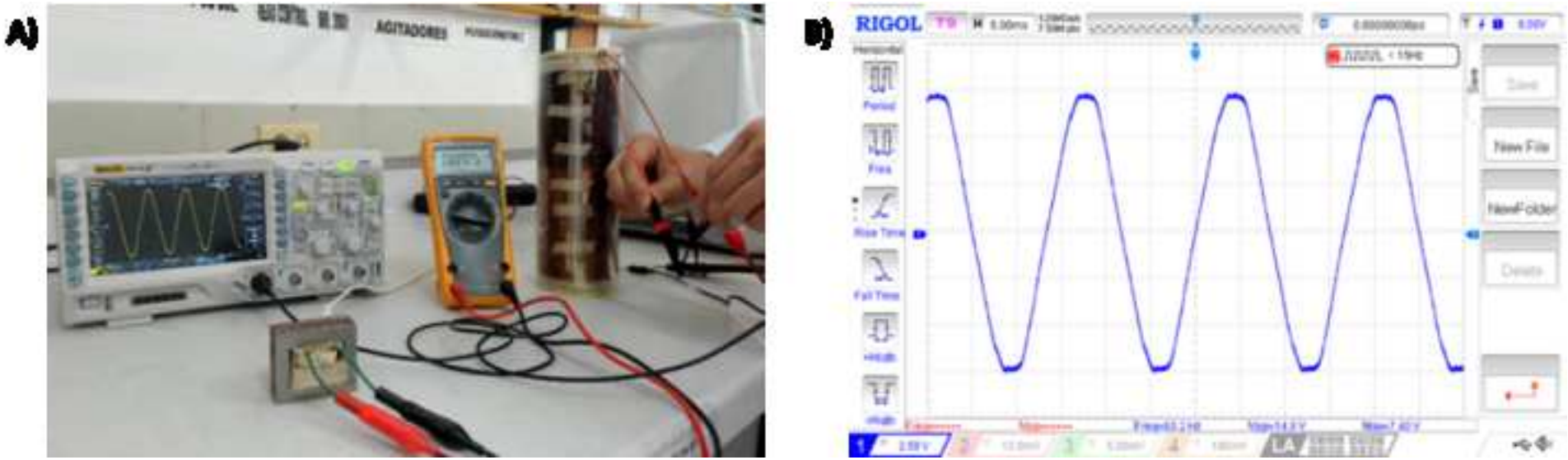

Table 1

System	Components	Width (mm)	Height (mm)
Electrical system	Air	100	100
	Electrodes	50	5
	Well-plate	7	20
	Hydrogel	3.5	3.5
	Culture media	6	8
Magnetic system	Air	500	600
	Coil	2	250

Table 2

System	Components	Relative Permittivity (ε)	Conductivity (σ)
Electrical system	Air	1	0
	Electrodes	1	1.73913 [MS/m]
	Well-plate	3.5	6.2E-9 [S/m]
	Hydrogel	8.03E+03	7.10E-2 [S/m]
	Culture media	2.67E+04	7.20E-2 [S/m]
Magnetic system	Coil	1	5.998E7[S/m]

Table of Materials

System	Name of Material/Equipment	Company	Catalog Number	Comments/Description	Quantity
Electrical stimulator	Operational amplifier	Motorola	LF-353N	----	1
	Resistors	----	----	22 kΩ	1
				10 kΩ	3
				2.6 kΩ	2
				2.2 kΩ	1
				1 kΩ	1
				220 Ω	2
				22 Ω	5
				10 Ω	1
				6.8 Ω	1
				3.3 Ω	2
	Polyester capacitors	----	----	1 nF	2
				100 nF	3
	VHF Band Amplifier Transistor JFET	Toshiba	2SK161	----	1
	Power transistor BJT NPN	Mospec	TIP 31C	----	1
	Zener diode	Microsemi	1N4148	----	1
	Switch	Toogle Switch	SPDT - T13	----	3
	Toroidal ferrite core	Caracol	----	T*22*14*8	1
	Cooper wire	Greenshine	----	AWG – 24	1
	Relimate header with female housing	ADAFRUIT	----	8 pin connectors	1
	Relimate header with female housing	ADAFRUIT	----	2 pin connectors	1
	Female plug terminal connector	JIALUN	----	4mm Lantern Plugs (Plug + Socket) 15 A	5
	Aluminum Heat Sink	AWIND	----	For TIP 31C transistor	1
	Led	CHANZON	----	5 mm red	1

	Integrated circuit socket connector	Te Electronics Co., Ltd.	----	Double row 8-pin DIP	1
	3 pin connectors set	STAR	----	JST PH 2.0	3
	2 pin screw connectors	STAR	----	For PCB	1
	3 pin screw connectors	STAR	----	For PCB	1
	Banana connector test lead	JIALUN	----	P1041 - 4 mm - 15 A	7
	Bullet connectors to banana plug charge lead	JIALUN	----	4 mm male-male/female-female adapters - 15 A	1
	Case	----	----	ABS	1
	Electrodes	----	----	Stainless – steel	2
	Electrode support	----	----	Teflon	2
	Printed circuit board			---	1
Magnetic stimulator	Cooper wire	Greenshine	----	AWG – 18	1
	AC power plugs	----	----	120 V AC – 60 Hz	1
	Banana female connector test lead	JIALUN	----	1Set Dual Injection - 4 mm – 15 A	2
	Banana male connector test lead	JIALUN	----	1Set Dual Injection - 4 mm 15 A	2
	Cell culture well plate support	----	----	PMMA	1
	Fuse	Bussmann	2A	----	1
	Transformer	----	----	1A – 6 V AC	1
	Tube	----	----	PVC	1
	Variable rheostat	MCP	BXS150	10 Ω	1
General equipment	Digital dual source	PeakTech	DG 1022Z	2 x 0 - 30 V / 0 - 5 A CC / 5 V / 3 A fijo	1
	Digital Oscilloscope	Rigol	DS1104Z Plus	100 MHz, bandwidth, 4 channels	1
	Digital multimeter	Fluke	F179	Voltage CC – CA (1000 V). Current CC – CA 10 A. Frequency 100 kHz	1

Reviewers' comments:

The authors want to thank the reviewers for their constructive comments. The manuscript has been thoroughly revised; thus, we believe it has greatly improved. Please note that corrections are highlighted in yellow within the manuscript.

Reviewer #1

Major Concerns:

1. In Figure 3:
1.1. In figure A), indicate where the electrodes are and in which region is the Distribution of EFs within the hydrogel, used in graph B).

R// We have indicated the electrodes and the hydrogel on figure 3A. Moreover, we added a red detail with the region of interest in figures 3B and 3D.

1.2. Are the y-axes of A) and C) correct? Shouldn't it be height (mm)?

R// We have modified the y-axes titles in figures 3A and 3C.

1.3. What are the units of the colour bars?

R// We have added the units of the colour bars in figures 3A and 3C.

1.4. It is not possible to understand in graph D) which region the Distribution of MFs is in the center of the coil of Figure C) was used, please indicate it.

R// We have added a red detail with the region of interest in figures 3B and 3D.

1.5. Is the x axis of D) correct? Shouldn't it be height (mm)? Adjust the x axis of figure D to the zero be in the center, do it similar to that of figure C.

R// We have changed the x-axis title in figure 3D and adjusted the x-axis to the zero be in the center.

Minor Concerns:
1) Is reference [43] correct? Where does it say that the capacitor acts as a short circuit at low frequencies?

R// It is our mistake. According to reference [43], the capacitive reactance is proportional to the inverse of the frequency. At higher frequencies, the capacitive reactance approaches zero, making a capacitor behave like a wire or a short circuit. At lower frequencies, the capacitive reactance approaches infinity, it acts as an open circuit. Therefore, we corrected the phrase in the manuscript.

"*Additionally, direct coupled stimulation cannot amplify high-frequency signals. The output tends to vary with time, generating supply voltage changes. It has little temperature stability, due to this its operating points change and at low frequencies the capacitor fails and acts as an open circuit [43].*"

2) Please, correct the phrase "In addition, a circuit was 433 designed to generate high voltages and frequencies between electrodes, creating different EFs 434 that overcome the limitations caused by the impedance of cell culture well-plates and air.", because circuit generates only one frequency.

R// Considering your comment, we have corrected the phrase within the manuscript.

"In addition, a circuit was designed to generate a frequency and high voltages between electrodes, creating different EFs that overcome the limitations caused by the impedance of cell culture well-plates and air."

3) Please, correct the phrase "464 [49]. To generate different type of signals, the operational amplifier can be replaced by a 465 monolithic function generator, which can produce high quality waveforms of high-stability and 466 accuracy. ", considering the circuit output transformer (figure 01) works with sine waves, but distorts other types of waves (square, triangular, sawtooth, ...)

R// Considering the circuit output transformer, we have corrected the phrase within the manuscript.

"To generate different type of signals, the operational amplifier can be replaced by a monolithic function generator, which can produce high quality waveforms of high-stability and accuracy with low amplitude, and the amplification stage can be replaced by a non-inverting operational amplifier or a stage with NPN transistors."

Reviewer #2

Major Concerns:
None

Minor Concerns:
1) In the first paragraph of the introduction, it would be good if the authors could comment on the disadvantage of using direct electrode stimulation while highlighting the benefits of non-invasive strategy to stimulate biological samples.

R// Considering your comment, we have modified the first paragraph of the introduction.

"Regarding the devices to generate EFs, direct coupling stimulators use electrodes that are in contact with biological samples in vitro or implanted directly into tissues of patients and animals in vivo[2], however, there are still limitations and deficiencies that include insufficient biocompatibility by the electrodes in contact, changes in the pH and molecular oxygen levels[1]. On the contrary, indirect coupling devices generate EFs between two electrodes, which are placed in parallel to biological samples[3], allowing a non-invasive alternative technique to stimulate biological samples and avoiding

direct contact between tissues and electrodes. This type of devices can be extrapolated to future clinical applications to perform procedures with a minimal invasion to the patient."

2) The second paragraph is too vague, as it just cites the examples of what others have done instead of focusing on what is lacking in their system and how your device tries to address these limitations.

R// We have mentioned the features of different electric field devices and the results of stimulation in the second paragraph of the introduction. The limitations are in the final paragraph of the introduction, and we wrote briefly how our protocol tries to address these limitations.

"Devices used by different authors have not considered either the adequate size of electrodes or correct length of the coil to homogeneously distribute both EFs and MFs. Furthermore, devices generate fixed voltages and frequencies, limiting their use to stimulate specific biological tissues. For this reason, in this protocol a computational simulation guideline is performed to simulate both capacitive systems and coils to ensure homogeneous distribution of EFs and MFs over biological samples, avoiding the edge effect. Additionally, it is shown the design of electronic circuits that generate voltages and frequency between electrodes and coil, creating EFs and MFs that will overcome the limitations caused by impedance of cell culture well-plates and air. These modifications will allow the creation of a non-invasive and adaptive bioreactors to stimulate any biological tissue."

3) In the methods, it will be better if the authors describe how the electrodes and wires will be sterilized before placing them in the incubator. Also, please mention the safety considerations to bear in mind when transferring/removing the setup from the incubator.

R// Considering your comment, we have mentioned how the electrodes and wires will be sterilized.

"2.1.8 Use an autoclave at 394.15 K (121 °C) for 30 minutes to sterilize the electrodes and use ultraviolet over night to sterilize the wires that are in contact with the incubator."

"2.2.7 Use ultraviolet over night to sterilize the wires that are in contact with the incubator. The coil is wrapped with transparent stretch film and use ethanol to sterilize the coil."

"2.1.10 Safety recommendations. To avoid any issue when transferring or removing the electrodes from the incubator make sure that cables are not tangled. Disconnect cables from the oscillator before removing the electrodes from the incubator. Never place the electrodes without the acrylic or Teflon supports."

2.2.10 Safety recommendations. To avoid any issue when transferring or removing the solenoid from the incubator make sure that cables are not tangled. Disconnect cables from the transformer before removing the solenoid from the incubator. Never place the solenoid without the PMMA support. Firmly grasp both PMMA support from the base and the solenoid when transferring or removing from the incubator.

4) In the discussion, it would be good, if the authors could comment on how this setup can be modified to function in an in vivo setting, such as for the stimulation of small/large animal models.

Considering your comment, in the discussion we added how this setup can be modified to function in an in vivo setting.

"Overall, this protocol is a useful tool which provides a technological contribution to the scientific community that works on biophysical stimulation of biological tissues. These devices will allow researchers to use EFs and MFs to stimulate the function of healthy biological tissues or those altered by a particular pathology. Considering this in further in vivo studies, different parameters and variables such as electrodes size, number of turns of the coil, stimuli strength and stimulation times would be determined to homogeneously distribute both EFs and MFs in animals such as pigs, calves, guinea pigs or rabbits. Additionally, bioreactors designed in this protocol can be extrapolated to clinical settings to improve regenerative techniques such as autologous cell implantation. Here, bioreactors can play an important role by stimulating biological samples, at the in vitro level, to improve the cellular and molecular features of cells, tissues and scaffolds before being implanted in the patient."

Editorial and production comments:

Changes to be made by the Author(s) regarding the written manuscript:

1. Please take this opportunity to thoroughly proofread the manuscript to ensure that there are no spelling or grammar issues.

R// The authors want to thank the editor for their constructive comments. The manuscript has been thoroughly revised; thus, we believe it has greatly improved.

2. Please revise the following lines to avoid previously published work: 49-52, 412-414, 419-421, 426-428.

R// Considering your comment, we modified the phrases in the manuscript. Please note that corrections are highlighted in yellow within the manuscript.

49-52
"This computational model is a promising tool that can modify parameters such as voltages, frequencies, tissue morphologies, well plate types, electrodes and coil size to estimate the EFs and MFs to achieve a cellular response."

412-414
"Considering the mentioned above, the combination of biomaterials, cell culture and external biophysical stimuli such as EFs and MFs, at in vitro level, has been introduced in tissue engineering as an alternative therapeutic technique to heal injured tissues."

419-421
"However, there are limitations such as alterations in biocompatibility of the cell culture medium by electrodes in contact, possible changes in pH and molecular oxygen levels."

426-428
"Considering these limitations, the second method was implemented, where external parallel electrodes were used. This indirect coupling system method has evidenced an increase in cell proliferation and molecular synthesis."

3. For in-text formatting, corresponding reference numbers should appear as numbered superscripts after the appropriate statement(s).

R// Considering your comment, we modified the reference numbers. Please see the manuscript.

4. The Protocol should be made up almost entirely of discrete steps without large paragraphs of text between sections. Please simplify the Protocol so that individual steps contain only 2-3 actions per step and a maximum of 4 sentences per step.

R// The protocol was modified so that individual steps contain few actions. However, some steps contain more than 2-3 actions because the steps have details to perform the computational simulation.

5. Please spell out the journal titles.

R// The journal titles were modified. Please see the manuscript.

Changes to be made by the Author(s) regarding the video:

1. As the narration and the written article are in English, can the screenshots (1:53, 6:18, etc.) be presented in English? If possible, please do so.

R// Unfortunately, the licensed software is in Spanish language, it is not possible to do this change.

2. Please increase the homogeneity between the video and the written manuscript. Ideally, all figures in the video would appear in the written manuscript and vice versa. The video and the written manuscript should be reflections of each other.

R// The figures in the written manuscript were added in the video.

3. Furthermore, please revise the narration to be more homogenous with the written manuscript. Ideally, the narration is a word for word reading of the written protocol.

R// Although video producers allowed to perform minor changes in the video, unfortunately, it is not possible to do this change because it requires to record our voices again and we do not have more financial resources to rent the equipment and produce the video again.

4. Add the title graphics for the speakers at the end, even though they spoke earlier.

R// The title graphics were added for the speakers at the end.